Spectral analysis of the non-proliferation experiment

Sjoerd de Ridder

ABSTRACT

To monitor a UN Test Ban Treaty, the US Department of Energy conducted a 1.5 kiloton chemical explosion at the Nevada Test Site, named the Non-Proliferation Experiment (NPE). I study a rarely known recording of the seismic waves of the NPE on a dense, transversely oriented array; the recording contains an extraordinary coda. The spectral information in this wavefield is analyzed to infer information about the subsurface. To first order, the energy arrives isotropically at the array. This allows for interferometric reconstruction of the direct wave between the receivers in the array.

INTRODUCTION

The US Department of Energy detonated a 1.5 kiloton chemical explosive charge at the Nevada Test Site at 12:01am on the 22nd of September 1993. This experiment, named the Non-Proliferation Experiment (NPE) was conducted in anticipation of the Comprehensive Test Ban Treaty approved by the United Nations in September 1996. The measurement was recorded by over 50 broadband seismic stations on the western United States (Tinker and Wallace, 1997). Scientists used these recordings and other measurements to learn to distinguish between nuclear and chemical explosions (Carr, 1994).

A less known and never published data set was recorded by the Subsurface Exploration Company of Pasadena, CA, which operated a 610-channel petroleum-exploration seismic array approximately 200 km distant in Railroad Valley (1). This sign-bit recording equipment was activated at midnight and recorded an extraordinary coda of over 10 minutes. This study reports an analysis of the first continuous 131 seconds of the recording, containing the first break and most of the coda energy.

The incoming waves are spatially coherent at early times, when all the energy comes in as one plane wave; while the incoming waves in the coda display a progressively more diverse range of angles. We will investigate how to use the information buried in a recording of such a distant source, by using processing techniques like cross-correlation.

DATA SET

The array was located approximately transverse to the direction of propagation. The station separation was 45 feet, and the array spans a length of over 7 km. The first 56 channels were cross-line to the other 553 stations oriented at N75E, and one channel was dead. There are 5 sign-bit recordings of 2^{14} samples at a sampling rate of 125Hz. There is less than a one second gap between each of the 5 recordings. The tape file was converted to an SEPLib file, and the above information was used to sort the headers. Two additional traces of the first recording were not found in the tape file, three traces were muted because their signals showed errors. Figures 2 to 5 contain time windows of the first recording for 512 stations (receivers 67 to 568). In a layered earth, all 609 channels would exhibit almost the same signal, because the array is approximately transverse to the direction of propagation. Clearly, from the difference in the observed signals along the array, the data set contains information about the lateral velocity variations in the earth.

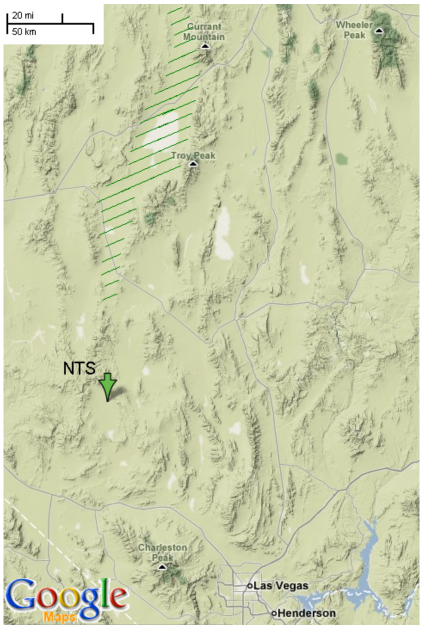

Figure 1: Map showing the location of Nevada Test Site (green arrow) and Railroad Valley (green shaded area). [**NR**]

SPECTRAL FILTERING OF THE RAW DATA

We first investigate the data in the frequency-wavenumber domain. The first break appears as a narrow line of energy through the origin, see left panel in Figure 6. It represents the spatial coherency and frequency content of the first arrivals that arrive directly from the source with limited multiple scattering in the medium. At later times scattered energy starts arriving from a compact range of angles, seen in Figures 6 and 7. These form a triangle containing all apparent slownesses of plane waves traveling along the array. The highest slownesses are of the plane waves that

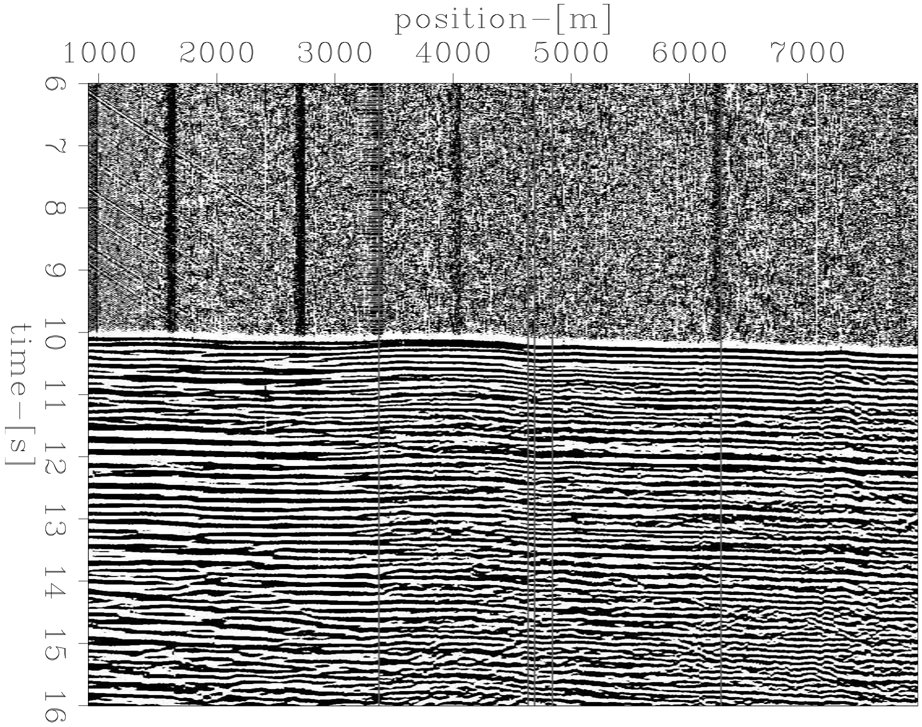

Figure 2: Black-white image of 10 seconds containing the first arrival. The arrivals are very coherent along the array. [**ER**]

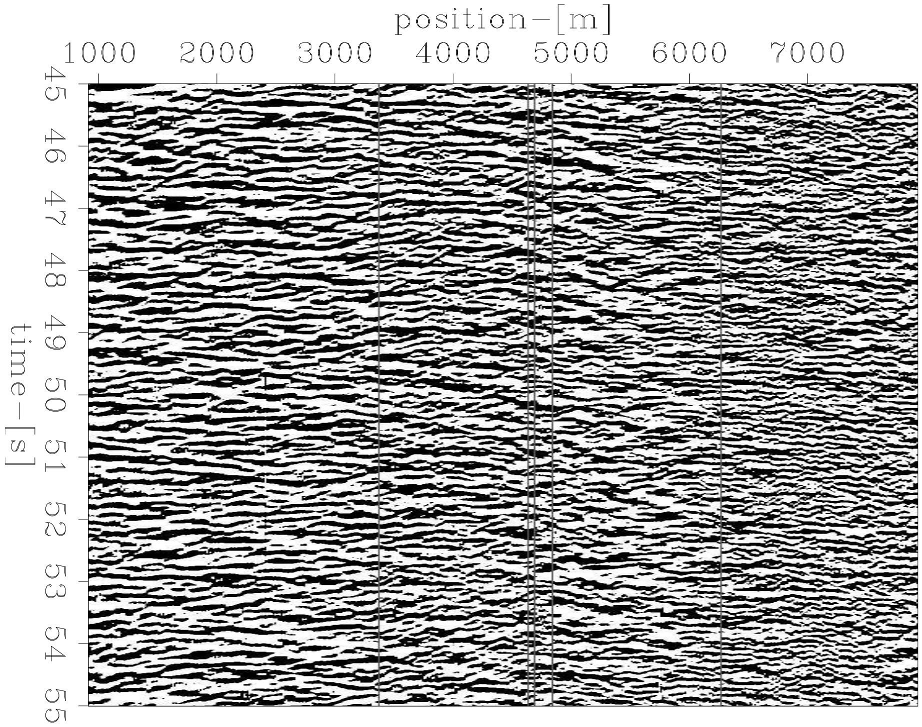

Figure 3: Black-white image of 10 seconds, 35 seconds after the first arrival. Events are incident from more angles than from purely transverse to the array. [**ER**]

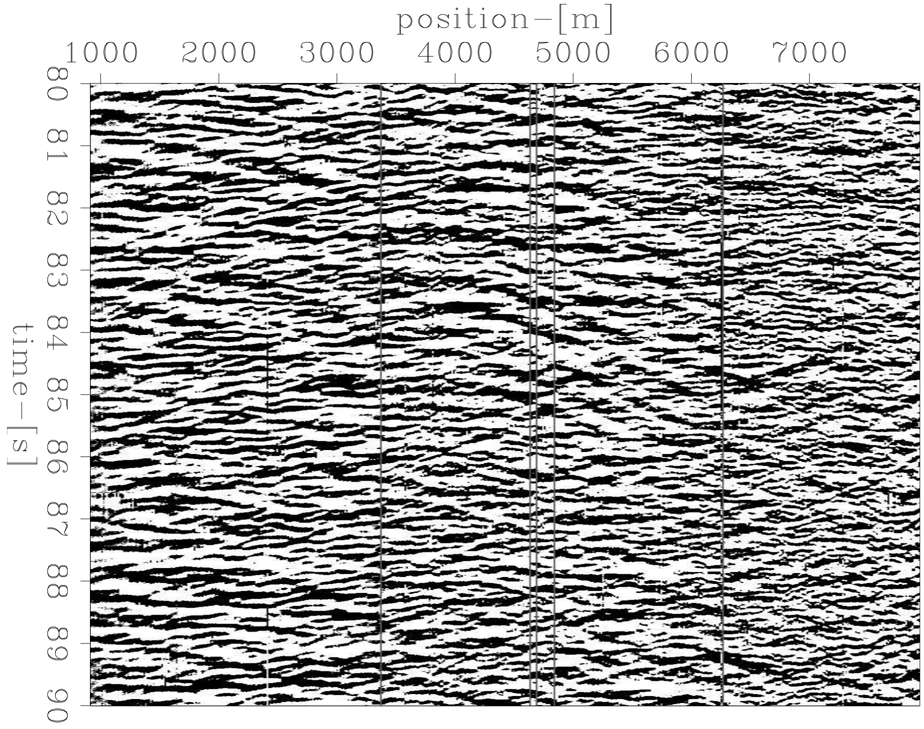

Figure 4: Black-white image of 10 seconds, 70 seconds after the first arrival. The high-frequency content becomes weaker than in Figure 2. [**ER**]

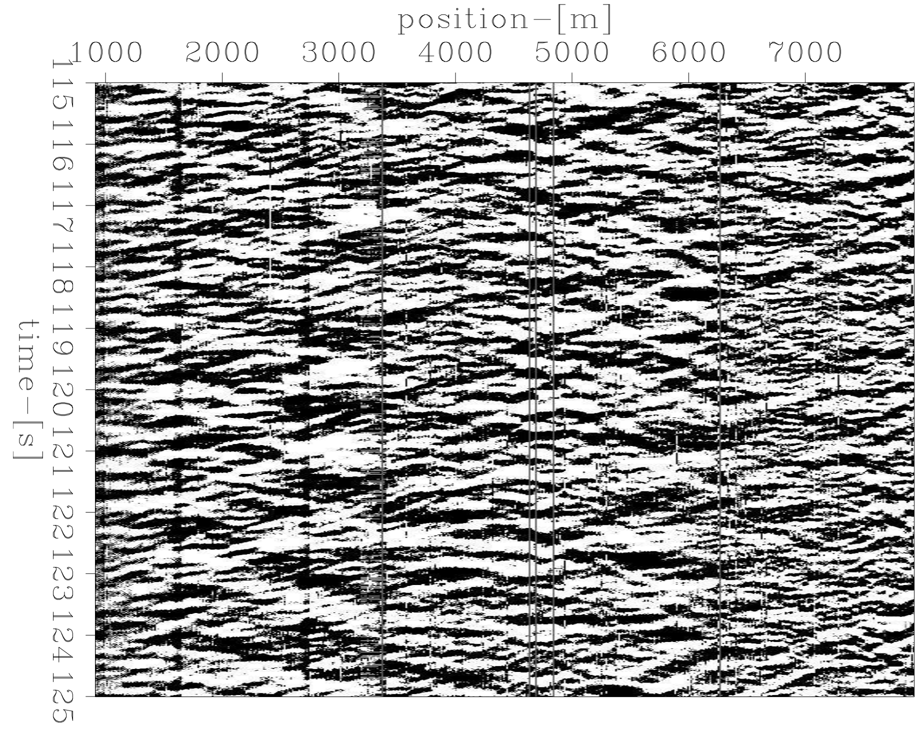

Figure 5: Black-white image of 10 seconds, 105 seconds after the first arrival. The high-frequency content becomes much weaker than in Figure 2. [**ER**]

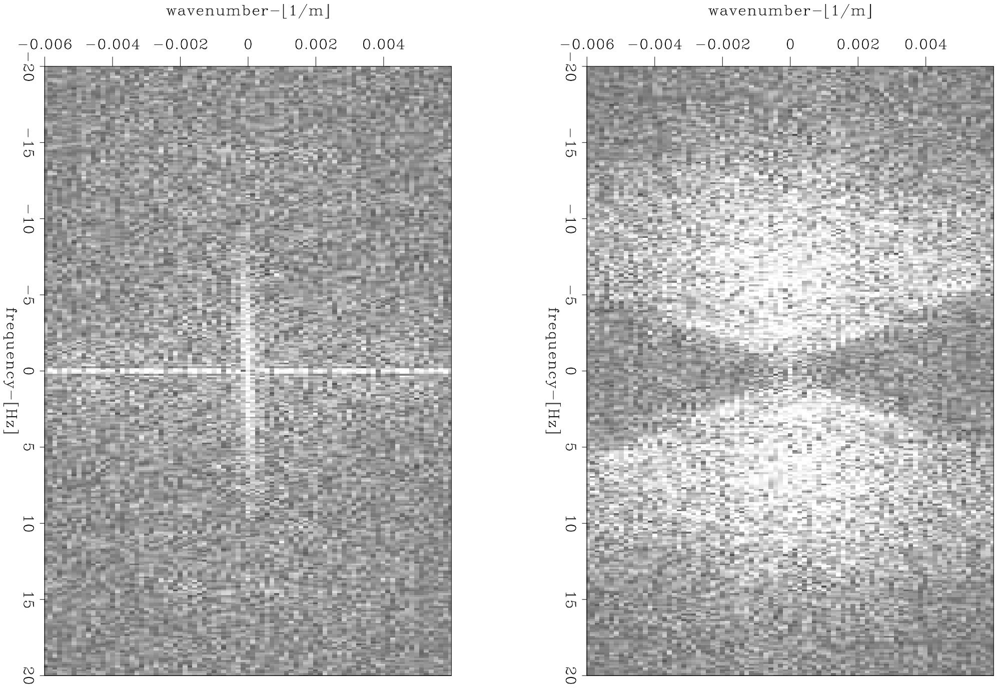

Figure 6: Frequency-wavenumber domain energy spectra of 4 second windows from the frames in Figures 2 and 3. Left panel: The spatial coherence along the array of the first arrival forms a delta function in space. Right panel: Already after 35 seconds a clearly defined cone shape is formed in slowness space. [**ER**]

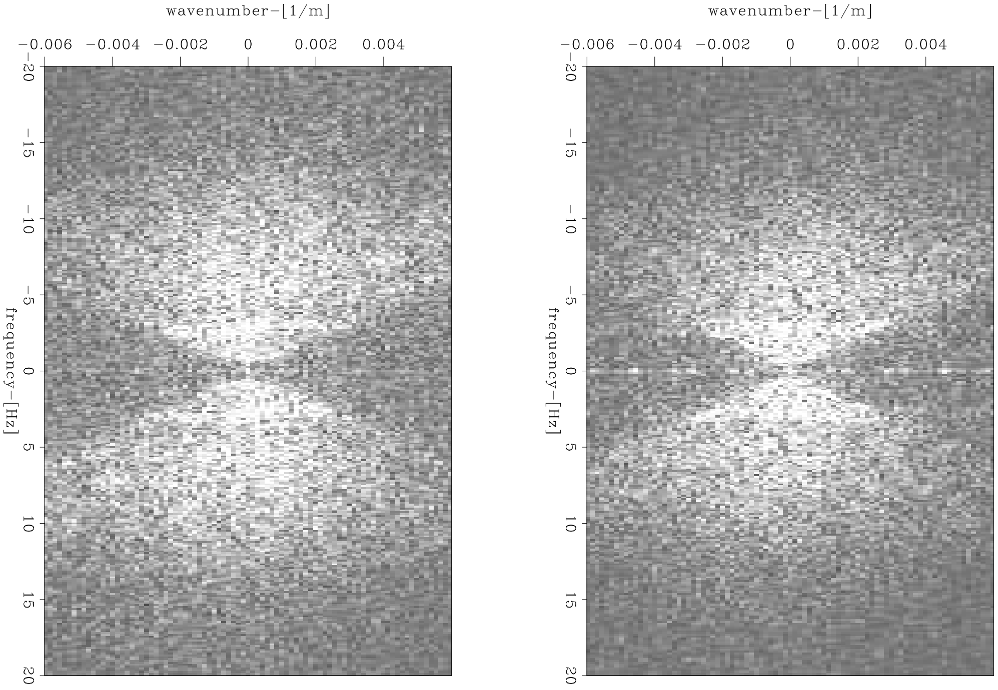

Figure 7: Frequency-wavenumber domain energy spectra of 4 second windows from the frames in Figures 4 and 5. Left panel: The cone persists for later times. Right panel: The power of the high-frequency content decreases. [**ER**]

travel purely along the receiver array. This angle is measured to be associated with an apparent velocity of $\frac{\omega}{k} = 770$ m/s. We apply a Butterworth low-pass filter on the angles in the frequency-wavenumber domain to filter for apparent velocities lower than $\frac{\omega}{k} = 770$ m/s. In addition, we apply a Butterworth low-pass filter to filter energy higher than 15 Hz. This process interpolates the zeroed traces and improved the overall appearance of the coda.

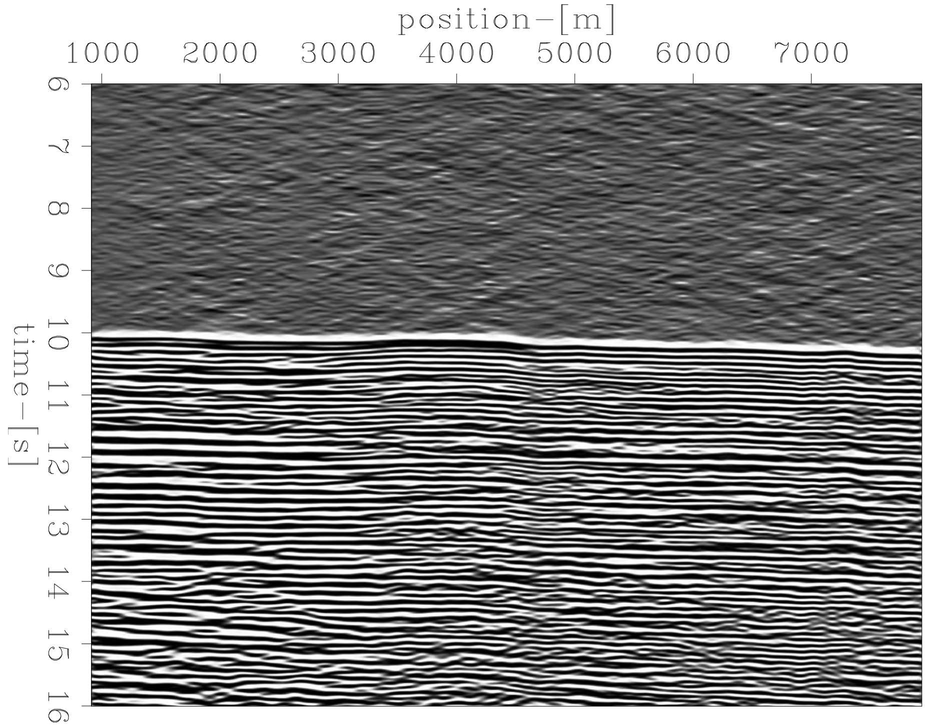

Figure 8: Gray-scale image of 10 seconds of the frequency-wavenumber filtered data containing the first arrival, compare to Figure 2. [**ER**]

INTERFEROMETRIC GREEN'S FUNCTION RETRIEVAL

Seismic interferometry is a novel geophysical tool to generate Green's functions by cross-correlations of the recorded background coda. Claerbout (1968) showed how the reflection response of a 1D medium can be retrieved from its transmission response. A general derivation for arbitrarily anisotropic and inhomogeneous media can be made through the reciprocity theorem of the time-correlation type (Wapenaar, 2003, 2004; Wapenaar and Fokkema, 2006). A reciprocity theorem interrelates two independent excitation states of a physical system in one and the same domain $\mathbb{D}$ (de Hoop, 1966; Fokkema and van den Berg, 1993). The key is to apply source-receiver reciprocity relations for the fields in the reciprocity theorem of the time-correlation type. Other derivations are based upon the diffusive character of the wavefield, (Weaver

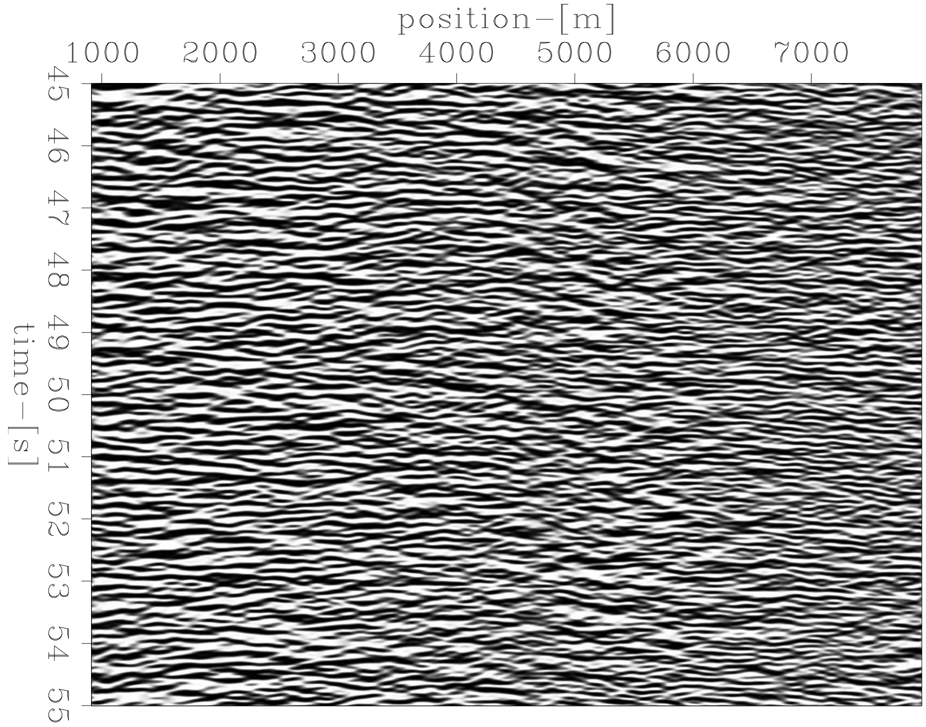

Figure 9: Gray-scale image of 10 seconds of the frequency-wavenumber filtered data, 35 seconds after the first arrival, compare to Figure 3. [**ER**]

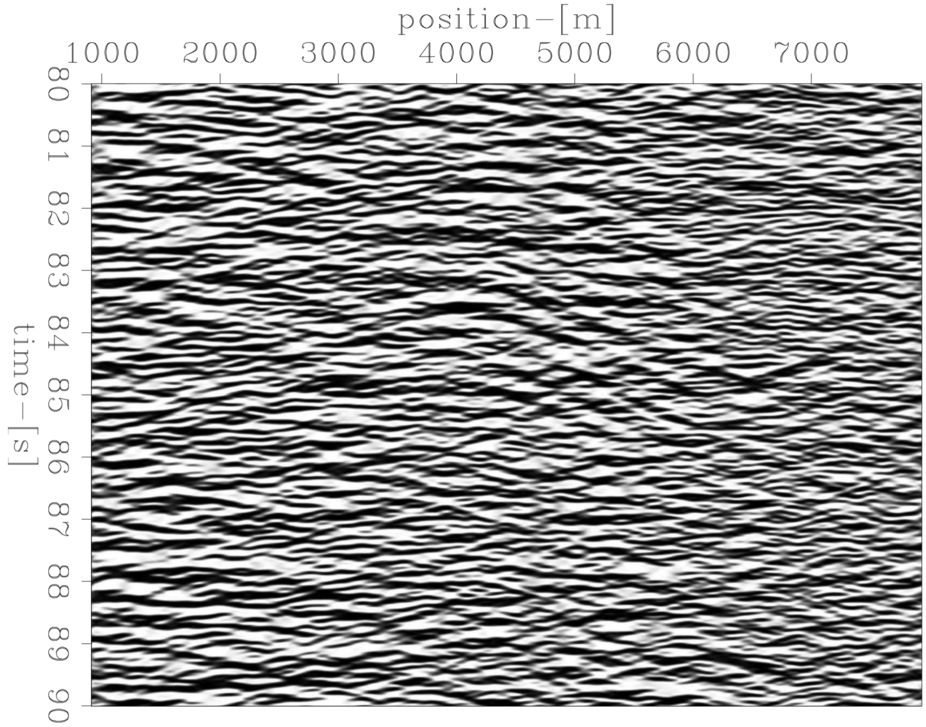

Figure 10: Gray-scale image of 10 seconds of the frequency-wavenumber filtered data, 70 seconds after the first arrival, compare to Figure 4. [**ER**]

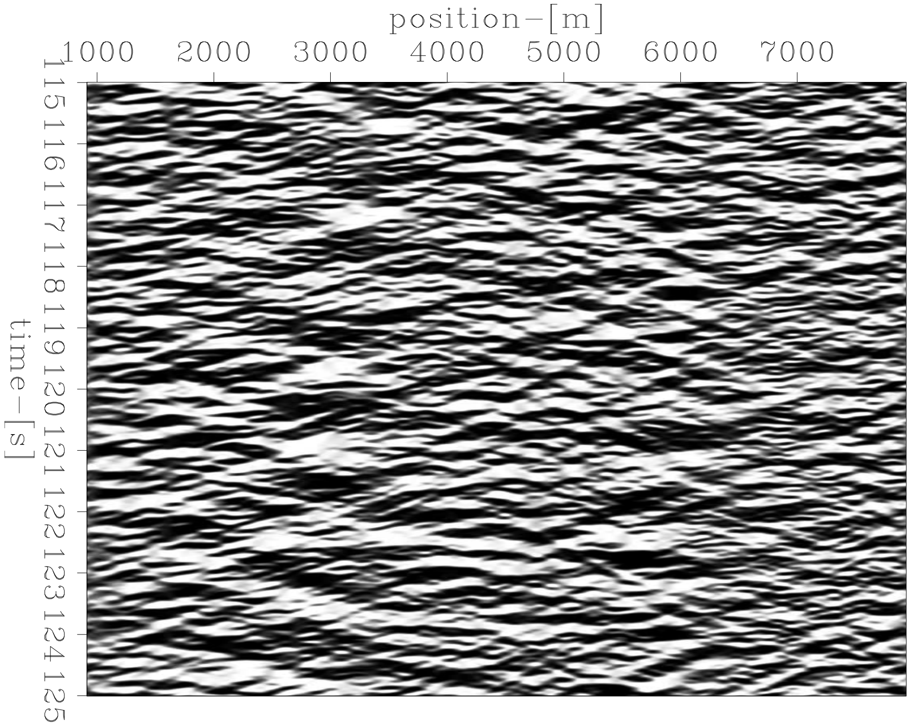

Figure 11: Gray-scale image of 10 seconds of the frequency-wavenumber filtered data, 105 seconds after the first arrival, compare to Figure 5. [**ER**]

and Lobkis, 2001, 2002; Shapiro and Campillo, 2004; Shapiro et al., 2005; Roux et al., 2005). The 3D equivalent of the 1D relation of Claerbout (1968), between the transmission coefficient T and the reflection coefficient R, proven by Wapenaar (2003), is

$$\begin{aligned}\hat{R}(\mathbf{x}_r,\mathbf{x}_s,\omega)+\hat{R}^*(\mathbf{x}_s,\mathbf{x}_r,\omega) &= -\oint_{\partial\mathbb{D}}\hat{T}(\mathbf{x}_r,x,\omega)\hat{T}^*(\mathbf{x}_s,x,\omega)\mathrm{d}^2x+\delta(\mathbf{x}_s-\mathbf{x}_r) \quad (1)\\ &\approx \left\langle \hat{T}(\mathbf{x}_r,..,\omega)\hat{T}^*(\mathbf{x}_s,..,\omega)\right\rangle \quad (2)\end{aligned}$$

written in the frequency domain, where ω denotes angular frequency, * denotes complex conjugation and $\langle\cdot\rangle$ denotes a time-average. The receiver station locations at $\mathbf{x}_r$ and $\mathbf{x}_s$ acquire the meaning of receiver and virtual source position in the retrieved reflection coefficients. The integral on the right-hand side of Equation 1 require individual recordings of sources positioned on a domain boundary $\partial\mathbb{D}$, enclosing the receiver stations and all heterogeneity. In ideal conditions this could be met by a time-averaging of recordings of sources, acting uncorrelated and positioned on the domain boundary.

The left-hand side of Equation 1 will be referred to as the retrieved Green's functions. We retrieve the superposition of a causal Green's function between $\mathbf{x}_s$ and $\mathbf{x}_r$ and the time reversed reciprocal Green's function between $\mathbf{x}_r$ and $\mathbf{x}_s$. In practice, we would recover these Green's functions convolved with the auto-correlation of an average source signal emitted by the source distribution (Wapenaar and Fokkema, 2006). The requirement of plane waves arriving isotropically from all directions is satisfied, to the first order. In practice not all contributions will be equally important: sources at stationary angles contribute dominantly to the retrieved result (Snieder, 2004; Snieder et al., 2006). For the recording of the NPE, we do not satisfy the conditions outlined above. Thus the retrieved Green's functions will be infested with spurious events with arrival times of non-existing interfaces (Dragonov et al., 2004; Snieder et al., 2006).

SYNTHESIS OF AN INTERFEROMETRIC SHOT GATHER

Although the NPE probably emits a spike-like source, the incident source spectrum is incident at the array from a wider range of angles, after multiple scattering, is unknown. After cross-correlation the receiver signals are deconvolved with an estimated source signal. The power spectra of the received signals are estimated using multitaper spectrum analysis codes from a library by Prieto et al. (2008). The procedure is as follows. The data is multiplied with a chosen number of Slepian tapers of increasing order; then a weighted average of the Fourier transformation is computed for each of the tapered data copies, resulting in a low variance estimate, while maintaining high resolution (Thomson, 1982; Prieto et al., 2007). One receiver is chosen as the 'master' receiver, and all other receivers are cross-correlated with this master, effectively turning this master receiver into a synthetic source. The source spectrum is estimated on the trace of the 'master' receiver using the multitaper estimation technique.

An example, choosing receiver number 400 as 'master' of a computed interferometric synthetic shot gather, is shown in the left panel of Figure 12. The first break arrives almost simultaneously at all receivers, and after cross-correlation appears as a strong spike with zero time lag. High frequencies are introduced because of the division with the estimated source spectrum. I apply a Butterworth low-pass filter to remove frequencies higher than 12 Hz, and the result is shown in the right panel of Figure 12. There are some interesting flat events at early and later times. These are however not appearing in the shot gathers synthesized for receivers further away from receiver number 400. We also retrieve a little bit of energy in the direct wave.

Most of the coherent energy between receiver stations along the array is associated with the direct wave from the synthetic shot to the receivers. We cannot identify any subsurface reflections. We see a spurious source at the right side of the synthetic shot gather. This could be caused by the correlation of the first break with the reflections from the side of the valley. We approximate our medium to have a 1D velocity structure, and we stack all the interferometric shot gathers that can be computed, by in turn selecting all 512 receivers as a 'master', with constant offset. All events from non-flat boundaries in the subsurface will destructively interfere. Thus we obtain a synthetic super-gather, in which only the direct arrival can be distinguished with certainty. The moveout of this event is estimated as approximately 1000 m/s, this is a reasonable velocity for ground roll.

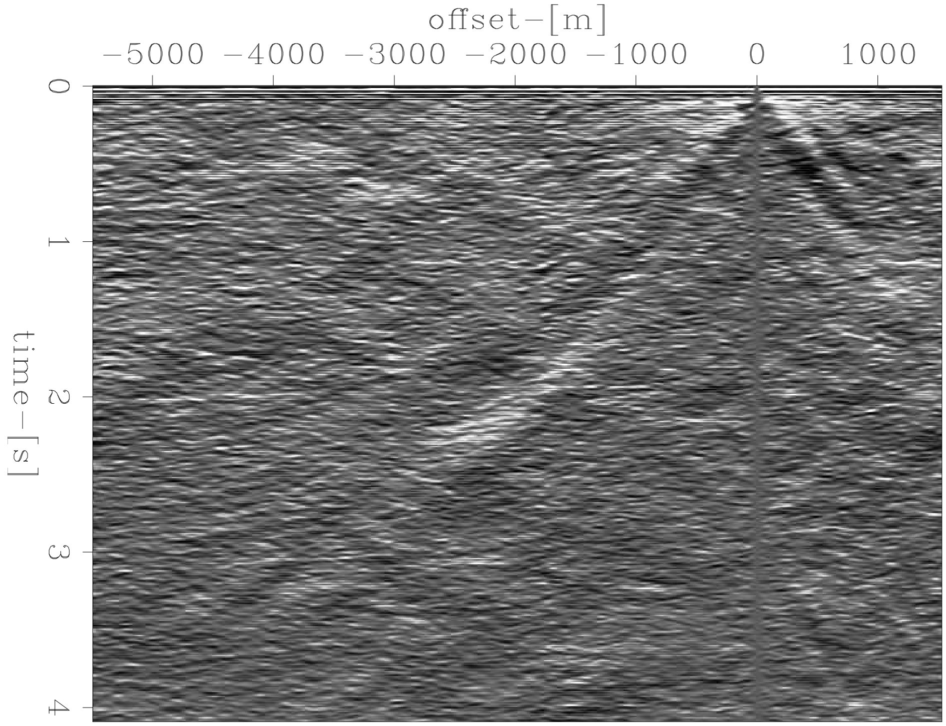

Figure 12: Interferometric shot gather with receiver number 400 as the master receiver. [**CR**]

CONCLUSIONS

We use the coda of a distant recording of the NPE containing multiple scattered waves incident at the array from a wide range of angles. We deconvolve for an estimated source spectrum. We discover that to first order, the waves are incident transverse isotropically to the array. The coherent energy between receivers is dominantly associated with the direct wave between receivers. To retrieve subsurface reflections, we need to sample the stationary phases of subsurface interfaces. For the direction of the array, these would lie approximately inline with and beneath the array, this is not in the dominant direction of propagation by the waves from the NPE.

ACKNOWLEDGMENTS

The author thanks Germán Prieto for many discussions on Green's function retrieval and for providing support for his multitaper spectrum analysis Fortran library, Jon Claerbout for discussions and encouragement to investigate this data set, Bob Clapp for writing the C routines that read the tape file, John Vidale for supplying the data tape file.

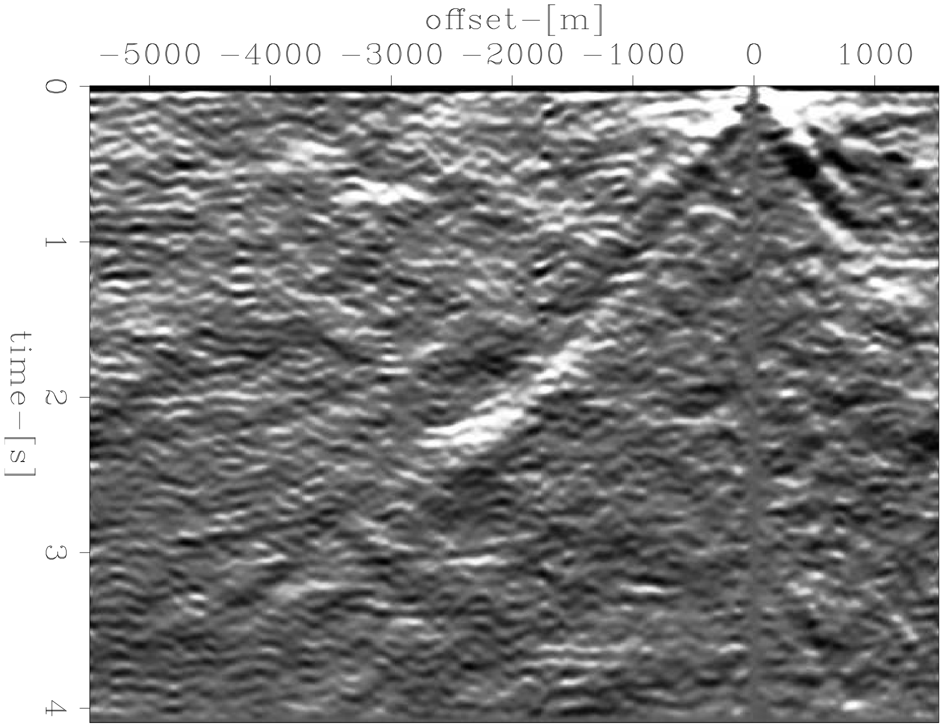

Figure 13: Interferometric shot gather with receiver number 400 as master receiver, low-pass Butterworth filtered for 12 Hz. [**CR**]

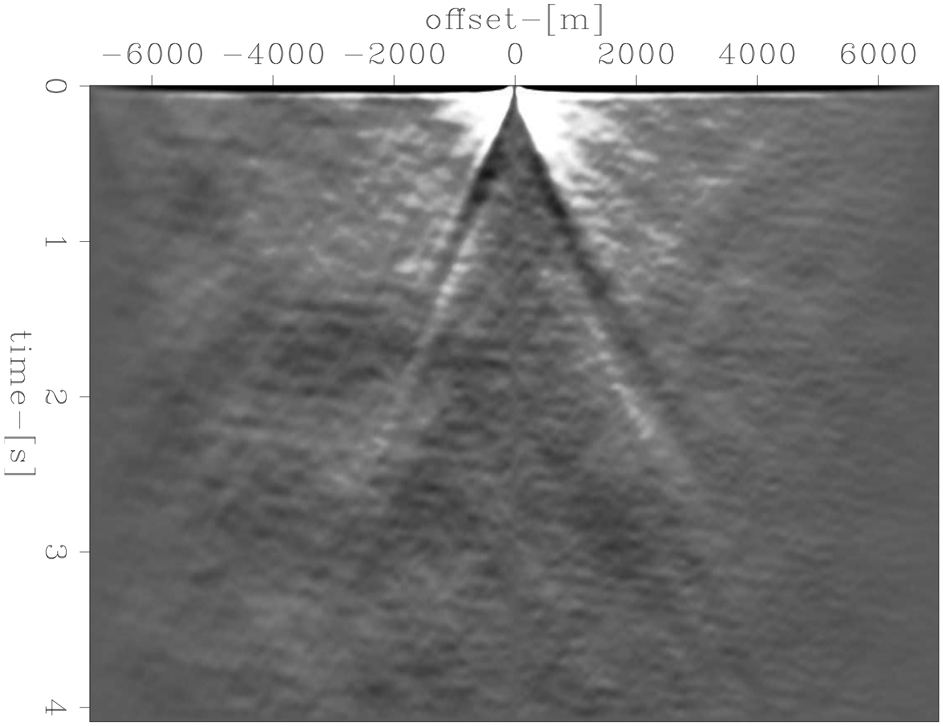

Figure 14: Interferometric super-gather, obtained by stacking cross-correlations of all possible receiver couples over common offsets. [**CR**]

REFERENCES

Carr, D. B., 1994, Non-proliferation experiment recorded at the pinedale seismic research facility: Sandia National Laboratories.

Claerbout, J. F., 1968, Synthesis of a layered medium from its acoustic transmission response: Geophysics, **33**, 264–269.

de Hoop, A. T., 1966, An elastodynamic reciprocity theorem for linear, viscoelastic media: Appl. Sci. Res., **16**, 39–45.

Dragonov, D., C. P. A. Wapenaar, and J. Thorbecke, 2004, Passive seismic imaging in the presence of white noise sources: The Leading Edge, **23**, 889–892.

Fokkema, J. T. and P. M. van den Berg, 1993, Seismic applications of acoustic reciprocity: Elsevier.

Prieto, G. A., R. L. Parker, and F. L. Vernon, 2008, A fortran 90 library for multitaper spectrum analysis. Submitted to Computers and Geosciences.

Prieto, G. A., D. J. Thomson, F. L. Vernon, P. M. Shearer, and R. L. Parker, 2007, Confidence intervals of earthquake source parameters.

Roux, P., K. G. Sabra, W. A. Kuperman, and A. Roux, 2005, Ambient noise cross correlation in free space: Theoretical approach: JASA, **117**, 79–84.

Shapiro, N. M. and M. Campillo, 2004, Emergence of broadband rayleigh waves from correlations of the ambient seismic noise: Geophys. Res. Let., **32**, L07614–1–L07614–4.

Shapiro, N. M., M. Campillo, L. Stehly, and M. R. Ritzwoller, 2005, High-resolution surface-wave tomography from ambient seismic noise: Science, **307**, 1615–1618.

Snieder, R., K. Wapenaar, and K. Larner, 2006, Spurious multiples in seismic interferometry of primaries: Geophysics, **71**, SI111–SI124.

Snieder, R. K., 2004, Extracting the green's function from the correlation of coda waves: A derivation based on stationary phase: Phys. Rev. E, **69**, 046610–1 – 046620–8.

Thomson, D. J., 1982, Spectrum estimation and harmonic analysis.

Tinker, M. A. and T. C. Wallace, 1997, Regional phase development of the non-proliferation experiment within the western united states.

Wapenaar, K., 2003, Synthesis of an inhomogeneous medium from its acoustic transmission response: Geophysics, **68**, 1756–1759.

———, 2004, Retrieving the elastodynamic green's function of an arbitrary inhomogeneous medium by cross correlation: Phys. Rev. Lett., **93**, 254301–1 – 254301–4.

Wapenaar, K. and J. Fokkema, 2006, Green's function representations for seismic interferometry: Geophysics, **71**, SI33–SI46.

Weaver, R. L. and O. I. Lobkis, 2001, Ultrasonics without a source: thermal fluctuation correlations at mhz frequencies.: Phys. Rev. Let., **87**, 134301–1 – 134301–4.

———, 2002, On the emergence of the green's function in the correlations of a diffuse field: pulse-echo using thermal phonons: Ultrasonics, **40**, 435–439.